
SMS
MEER

Photo credit: Nordinkraft

EMATS

EMATs for Thickness Gauging: Principle and Application

by Zhiyong Wang

The physical principle of generating and receiving ultrasound by electromagnetic acoustic transduction is explained, without the use of too many equations. The focus is on lorentz force, which is the mechanism for nonmagnetic materials. An example of normal beam shear wave is then used in thickness gauging.
—John Chen, Back to Basics Technical Editor

This paper reviews the operational principle of electromagnetic acoustic transducers (EMATs) for generating normal beam bulk waves and illustrates thickness gauging as an example of one application. Thickness gauging, using either conventional piezoelectric transducers or EMATs, has wide applications and is a well-established technique. The first commercial ultrasonic gauges were introduced in the late 1940s (Krautkrämer and Krautkrämer 1983), whereas EMAT-based gauges have been used for more than four decades. Thickness gauges based on either conventional or EMAT ultrasonic principles are available commercially.

In an EMAT, a set of wires, usually in the form of a coil, is placed in a magnetic field near a conducting or ferromagnetic object. A pulse of current flowing through the coil produces a burst of ultrasonic energy in the material. Since EMATs rely on electromagnetic induction across a small gap to generate and detect ultrasonic waves in the material, they eliminate the need for a couplant, and are especially suitable for applications involving relative motion between the inspection device and the specimen and the inspection of objects with elevated temperature. EMATs have been successfully applied to field scenarios where considerable scan speed and unprepared, rough, rusty surfaces are common. In an EMAT nondestructive testing system, the ultrasound is generated directly at the surface of the test object itself. Unlike piezoelectric transducers, a slight tilt of the probe does not change the direction in which the ultrasound is generated and does not distort echoes, meaning accurate readings are maintained.

When reflected from the metal surface, the elastic wave moves the particles back and forth in the magnetic field . . .

A good understanding of the coupling mechanism is indispensable for optimal design and best use of EMAT systems. In general, there can be three contributions to the electromechanical coupling of an EMAT: namely, contributions due to lorentz force, magnetization force, and magnetostrictive force (Thompson 1990). Lorentz force mechanism arises in all conducting materials, whereas the other two mechanisms occur only in ferromagnetic materials. In this paper, we solely consider lorentz force since it is the only coupling mechanism in nonmagnetic metals and is also the dominant coupling mechanism in magnetic metals when the magnetic field is near or above saturation.

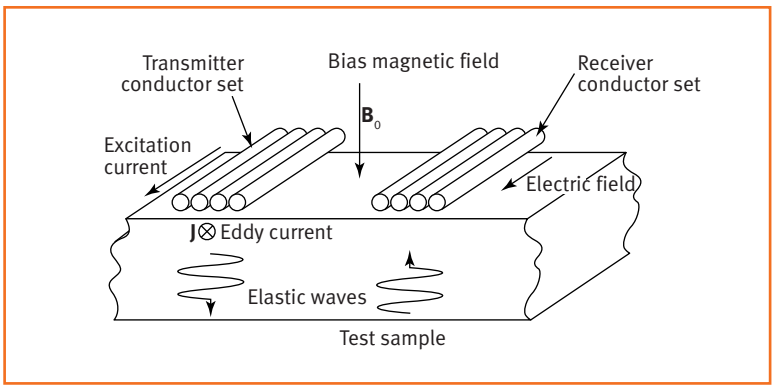

Figure 1. Representation of a general lorentz force EMAT consisting of transmitter and receiver conductor sets placed in a bias magnetic field near a metallic test sample (adapted from Maxfield and Wang 2018 with permission).

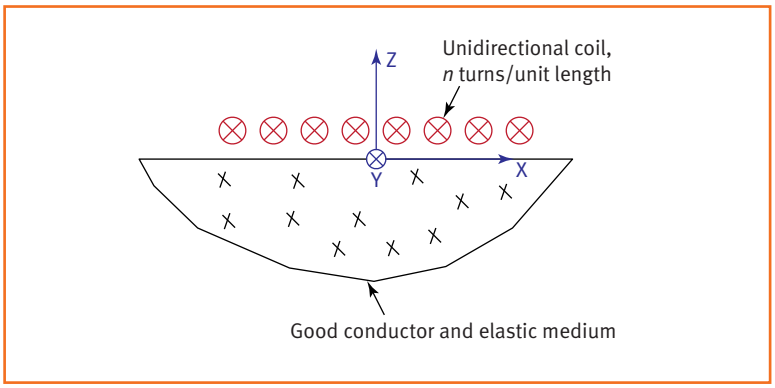

Figure 2. Unidirectional coil above bulk metal surface.

The left side of Figure 1 illustrates how an EMAT transmitter works. When a transmitter coil is placed near a metal, a time-varying current flowing through the coil induces eddy current density **J** in the near-surface region of the metal. This induced current interacts with the bias magnetic field $\mathbf{B}_0$, causing a lorentz body force $\mathbf{f} = \mathbf{J} \times \mathbf{B}_0$ that is transferred to the lattice of the metal and launches elastic waves into the material. The right side of Figure 1 shows how an EMAT receiver operates. When reflected from the metal surface, the elastic wave moves the particles back and forth in the magnetic field, giving rise to an electric field that generates an eddy current in the metal. This eddy current, in turn, induces a voltage in the receiver coil placed near the surface by electromagnetic induction.

Generation Mechanism

This section explains the generation mechanism based on lorentz force. Figure 2 shows an infinitely wide unidirecitonal coil placed above a good conductor that is also an elastic medium occupying the lower half space. For ease of reference, a coordinate system is established with the X-axis parallel to the metal surface, the Y-axis parallel to the coil currents and pointing into the page, and the Z-axis being the outward normal of the metal surface.

Governing Equations

For lorentz force EMATs, the governing equations consist of Maxwell's equations, which describe the relation between electromagnetic quantities, and Navier's equation, which is an elastodynamic equation in terms of particle displacement. These are partial differential equations subject to electromagnetic and elastic boundary conditions at the surface of the material. Due to relatively weak coupling between the

electromagnetic and elastic fields in an EMAT, the modeling problem can be solved in sequential steps that compute the induced currents, the bias magnetic flux density, the resulting lorentz body force, and the radiated elastic fields (Thompson 1990).

The analysis starts with Faraday's law of induction and Ampere's law, which describe the relation between electric and magnetic field quantities. The displacement current appears as a term in the Ampere's law equation. For EMAT applications, the frequency is typically no more than 100 MHz. As a result, the conduction current is about $10^8 \times$ higher than the displacement current. Thus, we can ignore the displacement current. For simplicity, we further assume that all magnetic, electric, and elastic properties of the metal are homogeneous (constant with position), linear (invariant with field intensity), and isotropic (constant with field orientation).

Induced Currents and Dynamic Fields

The current in the transmitter coil induces eddy currents and dynamic fields in the near-surface region of the metal. Incorporating the constitutive relation and Ohm's law into the previous equations, we get a new set of equations in terms of induced current and magnetic field. It is assumed that the induced current has only a *y*-component (parallel to the current direction in the coil conductors) that varies only with penetration into the metal. Symmetry tells us that there is only an *x*-component of the time-varying magnetic field, also varying only with penetration. An approximate procedure of determining the magnetic field at the metal surface starts by replacing the real metal that has a large but finite conductivity with a perfect conductor, where the dynamic fields must be fully shielded from the perfect conductor's interior. This means that the current sheet induced in the metal surface is equal in magnitude to the excitation current sheet in the coil but in the opposite direction. It follows that the surface time-varying magnetic field is also equal to the current sheet in magnitude and points in the negative X-direction. Here, the dynamic magnetic field has the contributions from both the coil current and the image current. We then assume that the surface magnetic field retains this value in a real metal.

The solution to these electromagnetic equations reveals that the intensity of the induced current and the magnetic field decays exponentially with increasing penetration. At a distance

$$\delta = \sqrt{\frac{2}{\omega\sigma\mu}} \tag{1}$$

into the material, their amplitude decreases to about 37% of the value at the surface. This distance is the classical skin depth. Here, ω (=$2\pi f$) is the angular frequency in radian/s, σ is the conductivity in siemens/m, and μ is the permeability in henry/m. Although the preceding analysis is derived from currents in a half-space, it remains valid for a current distribution in any conductor whose radius of curvature is much larger than the skin depth. Note that the integral of the body current density over depth equals the aforementioned surface current sheet, which is the image of the excitation current sheet. This is required to fully shield the interior of the metal from dynamic electromagnetic fields.

Lorentz Body Force

We consider a case where the static magnetic field lies in the X-Z plane having components along the X- and Z-directions. As a result, the lorentz body force has *x* and *z* components that are products of the induced current density and the respective *z* and *x* magnetic field components. This lorentz force mechanism is the same as what drives an electric motor, which converts electrical currents into mechanical forces.

Solution to Wave Equations for Plane Wave Case

The wave equation can be derived from the general Navier's equation by noting that all quantities do not vary in the X- or Y-direction and particle displacement only occurs in the X-Z plane. A normal bias magnetic field generates an in-plane lorentz force that launches shear waves into the elastic material, while a parallel magnetic field generates an out-of-plane lorentz force that launches longitudinal waves. In both cases, the displacement occurs in the direction of the driving lorentz force.

In addition to the wave equation, there are also boundary conditions to be satisfied. For a stress-free material surface, we need to make sure that the stress components on the surface are zero. The theory of elasticity is used to translate these boundary conditions into requirements on displacement. We can now make a guess that the solution in particle displacement takes a certain form determined by the driving lorentz force. The unknown coefficients are then obtained by substituting the postulated solution back into the wave equation and the boundary conditions. The final solution includes a particular solution representing a localized deformation that decays in space at the same rate as the induced eddy currents. The other term in the solution is the homogeneous solution. This is the wave motion that propagates away from the material surface and carries energy into the interior.

Parameter β

The analytical expression of the final solution suggests that we can define a parameter β as

$$\beta = \frac{\delta^2 k^2}{2} \quad (2)$$

where

δ is the skin depth defined in Equation 1, and
$k = 2\pi/\lambda$ is the wave number, with λ being the wavelength of the elastic wave.

This parameter, which couples the electrical and magnetic properties of the material (σ and μ in Equation 1) with the elastic properties of the material, enters into the EMAT coupling efficiency. Equation 2 and the definition of *k* show that β is determined by the ratio of the electromagnetic skin depth to the wavelength of the elastic wave that is generated. Thus, β is a measure of how electromagnetic forces that drive elastic displacements are distributed over the elastic wavelength. Small β means that the driving force is concentrated within a region beneath the metal surface that is thin compared to the elastic wavelength. This is the only parameter that couples the electromagnetic and elastic properties of the metal. From Equations 1 and 2, we know that β is small at low frequencies and grows proportionally as the frequency increases. The expression of the solution tells us that the displacement is independent of β for small β (meaning, $\beta \ll 1$) and decreases with increasing β. This is not an issue for carbon steels since they have high permeability, making the skin depth small compared to elastic wavelength for a large range of frequencies. The value of β is about 0.30 for 20 MHz shear waves in most aluminum alloys, and is about 0.40 for 1.0 MHz shear waves in nonmagnetic stainless steels. These frequencies represent roughly a preferred range of frequency values for these materials, which ensures the high conductivity limit is valid and the EMAT efficiency is not lowered by a large β. As β is greater than unity, the EMAT efficiency decreases very significantly.

Reception Mechanism

In the reception process, elastic energy in the metal is converted into electromagnetic energy in the receiver coil circuit, analogous to the operation of an electrical generator. To have a direct and simplified explanation of how EMATs receive elastic waves, we can consider a case where the receiver conductors are massless conducting strips that are bonded to the metal surface and connected electrically in a series. When a shear wave gets reflected by the surface, the particles move in a direction perpendicular to the strip. This causes the strips to move back and forth in the bias magnetic field. The charges in the moving conductor experience a magnetic lorentz force that is proportional to the particle velocity. This force generates an electric field. The open circuit voltage developed in the receiver coil is the line integral of this electric field along those portions of the strip that are illuminated by the beam.

The charges in the moving conductor experience a magnetic lorentz force that is proportional to the particle velocity.

Transfer Impedance

The previous sections cover the generation of elastic displacements in the metal surface by a time-varying current in the transmitter coil and the reception of a voltage induced in the receiver coil after the elastic wave propagates over some distance and gets reflected by that surface. One way to describe the total EMAT response is very useful when analyzing how to best incorporate an EMAT into an actual measurement circuit. The transfer impedance is defined as the open circuit voltage in the receiver coil divided by the current through the transmitter coil and can be broken into four independent terms (Maxfield and Wang 2018):

- Intrinsic transfer impedance, calculated in the high conductivity limit and not incorporating any effects of liftoff due to coil or magnet. Factors considered in this term include coil winding density and bias

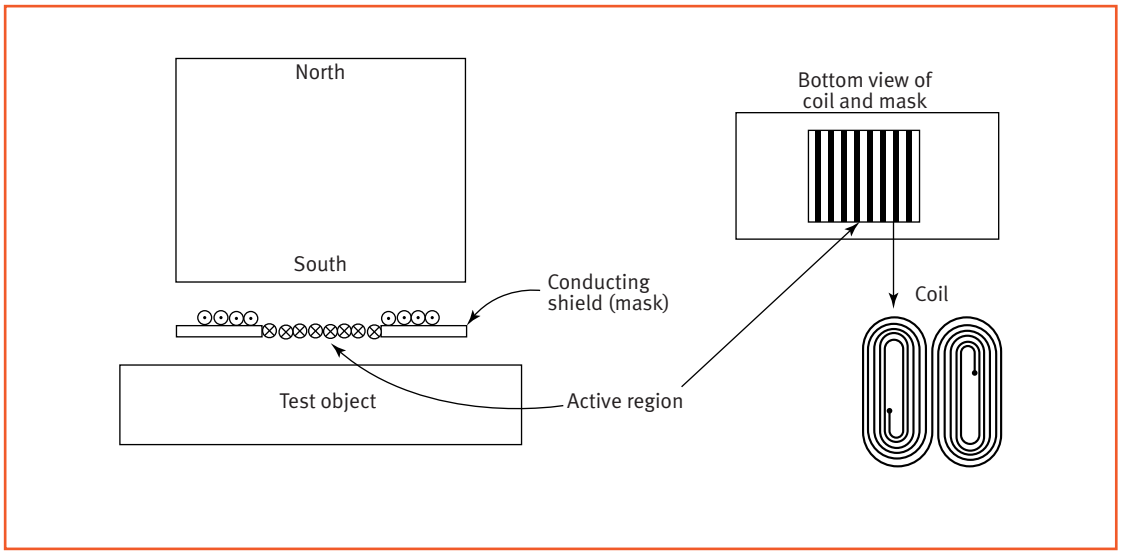

Figure 3. A normal beam shear wave EMAT (not to scale).

magnetic induction of transmitter and receiver, and illuminated length and width of the receiver coil.

- Magnet liftoff coefficient
- Coil liftoff coefficient
- Factor that represents the effects of finite conductivity. $F(\beta) = 1/(1 + \beta^2)$ is an exact expression for normal beam shear and longitudinal waves.

The transfer impedance can be used to estimate the EMAT signals for cases such as backwall reflection of the normal beam shear or longitudinal waves. Factors such as nonuniformity of the bias magnetic field, beam spread, and attenuation are neglected.

An EMAT for Generating Normal Beam Shear Waves

Major Components

Figure 3 shows the major components of a typical EMAT for generating and receiving normal beam shear waves. The permanent magnet generates a static bias field that is primarily perpendicular to the metal surface beneath the active region marked in the figure. This normal field is relatively uniform over a region around the center of the magnet and is responsible for producing the in-plane lorentz force on the induced current at the metal surface. The coil has a shape resembling two racetracks connected at the center, with the central conductors carrying currents flowing in the same direction. This coil serves as a practical approximation to the uniformly polarized current sheet discussed in the previous sections. A conducting mask with a rectangular window at the center is used to shield the return currents in the coil from the test object, hence defining the beam aperture.

Very often, a backing iron made of soft iron or cold rolled steel is included at the backside of the permanent magnet to enhance the magnetic flux density in the magnet as well as at the metal surface. When testing magnetic objects, a pole cap made of the same material as the backing iron is usually placed at the front face of the magnet to further concentrate the flux and create a stronger field that improves the efficiency of elastic wave generation and reception.

Illustrative Results from Simulation

Simulations based on the finite element method (FEM) have been widely employed to better understand the process of elastic wave generation by EMATs. The normal beam shear wave EMAT illustrated in Figure 3 has been simulated in an FEM software using the perpendicular induction current mode of its AC/DC module and the plane-strain mode of its structural mechanics module. Various quantities in the cross section of the test object perpendicular to the coil current were calculated. The geometrical and physical symmetry of the system allows simulating only half of the entire system, as shown in Figure 4. The test object is a steel plate that is 16 mm thick and 160 mm long. The material is mild steel with a Young's modulus of 200 GPa, Poisson's ratio of 0.29, and density of 7.85×10^3 kg/m^3. This combination of parameters gives a shear velocity of 3.14 mm/μs. The conductivity of the steel is 7×10^6 S/m, and the relative permeability is 100. The excitation current is a

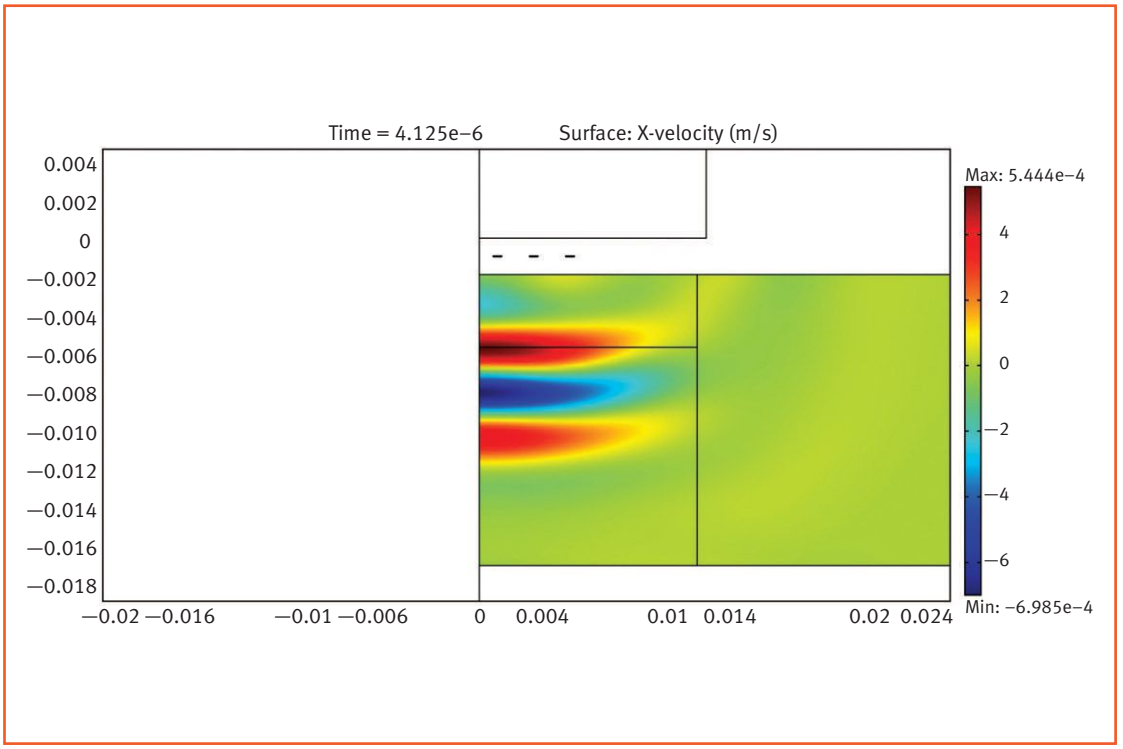

Figure 4. In-plane particle velocity (in X-direction) in the cross section of the test object.

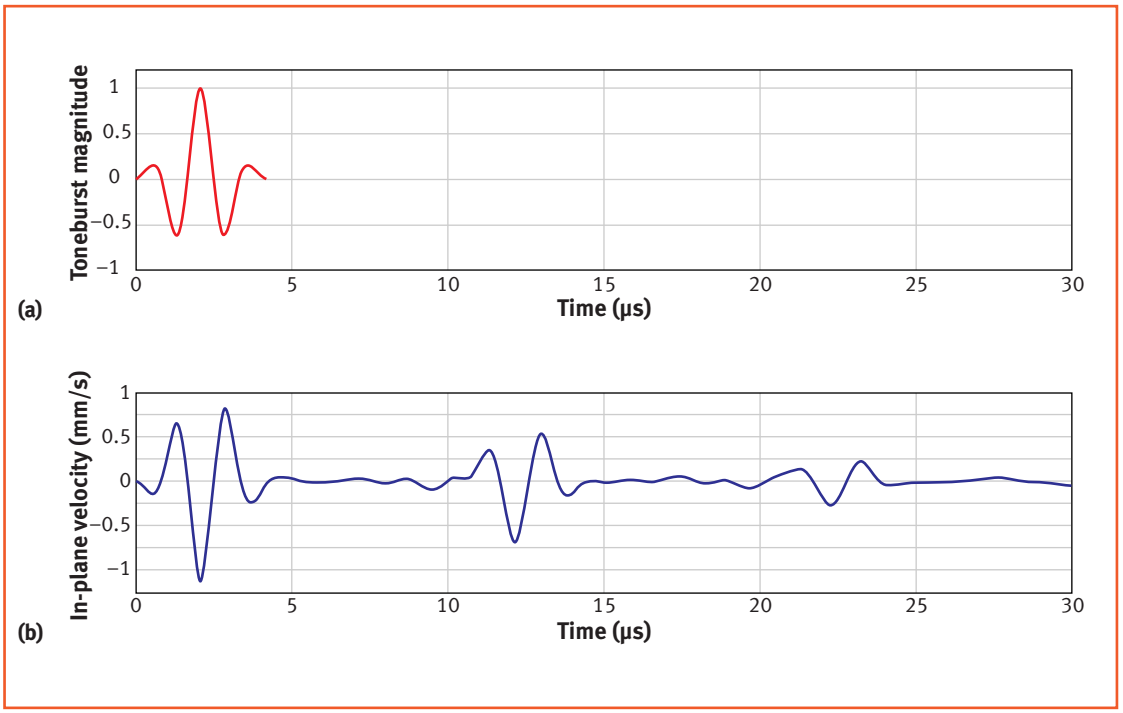

Figure 5. Waveforms of the excitation current flowing through the coil and the calculated particle velocity at the upper surface of the test object: (a) the toneburst excitation used in simulation (normalized); and (b) the calculated in-plane particle velocity under the center of the transmitter.

600 KHz tone burst with 2.5 cycles and has a magnitude of 100 A (see Figure 5). The toneburst is modulated by a hanning window. The mesh size within the plate is 0.2 mm × 0.2 mm (about 1/26 of the shear wavelength). A transient (time dependent) analysis was performed using a step size of 0.025 μs (about 1/66 of excitation period).

Figure 4 shows a snapshot of the horizontal particle velocity at the end of the toneburst, meaning t = 2.5 excitation periods. Two peaks (in red) and one trough (in blue) are clearly seen, which produce the "first signal" between 0 and 4.2 μs as shown in Figure 5 when propagating away from the surface. The beam spread and nonplanar wavefront due to finite transducer size are also visible in Figure 4.

In EMAT thickness gauging, the transit time technique usually involves measuring the time interval between two successive backwall echoes, similar to the "Mode 3" measurement technique commonly known for delay line or immersion piezoelectric transducers. From the signal in Figure 5, the transit time is calculated to be 10.075 μs. This gives a thickness of 15.83 mm, giving a relative error of about 1%. Since the second echo is roughly a shifted and scaled version of the first pulse, the technique of cross-correlation can be employed to automate the extraction of the transit time. Accuracy above the limitation of the sampling period (in this case, 0.025 μs) can be achieved with the help of curve fitting around the peak of the cross-correlation result.

Through-Thickness Resonance

For bulk waves, through-thickness resonance occurs when the transmitted signal is at some special frequency determined by the wave speed and material thickness and has enough number of cycles such that after repeated reflections between material boundaries, the received signals are coherently overlapped because of constructive interference, giving a sharp response in the magnitude spectrum. Taking shear wave as an example, the relationship between resonance frequency and material thickness can be derived by assuming two shear waves traveling in opposite directions (Figure 6) and imposing stress-free boundary conditions on the top and bottom surfaces of the plate.

The relationship between the resonance frequency f and the plate thickness d is

$$f = n\left(\frac{C_S}{2d}\right) \quad (3)$$

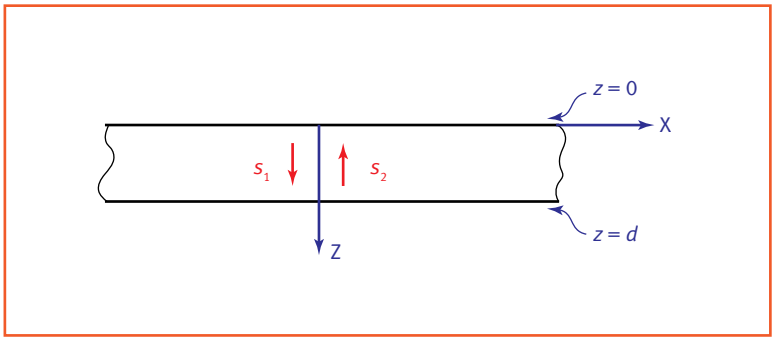

Figure 6. Normal beam shear waves (S_1 and S_2) traveling in upward and downward directions.

The resonance frequency interval in terms of shear wave speed and plate thickness is

$$\Delta f = \frac{C_S}{2d} \quad (4)$$

where

C_S is the shear velocity.

It can be seen that this resonance frequency interval (Δf) is the reciprocal of the transit time (Δt) it would take an elastic wave to traverse twice the thickness,

$$\Delta t = \frac{2d}{C_S} \quad (5)$$

Equations 4 and 5 indicate that very thin material will be a challenge for both transit time (time domain) and resonance (frequency domain) techniques due to requirements on finer time resolution and higher sampling frequency. This is partly mitigated by utilizing shear waves instead of longitudinal waves in thickness gauging since the shear velocity is about half of the velocity of longitudinal waves for most metals.

The resonance technique is usually less accurate using piezoelectric transducers, as compared to using EMATs, due to variations in couplant thickness, tilting of the piezo transducer, and the energy leakage caused by stronger coupling between the piezo transducer and the sample.

Typical Application

Normal beam shear wave signals were collected on a 5.29 mm steel plate using the EMAT shown in Figure 3. The shear velocity of the steel was found to be C_S = 3.240 mm/μs on a calibration plate with

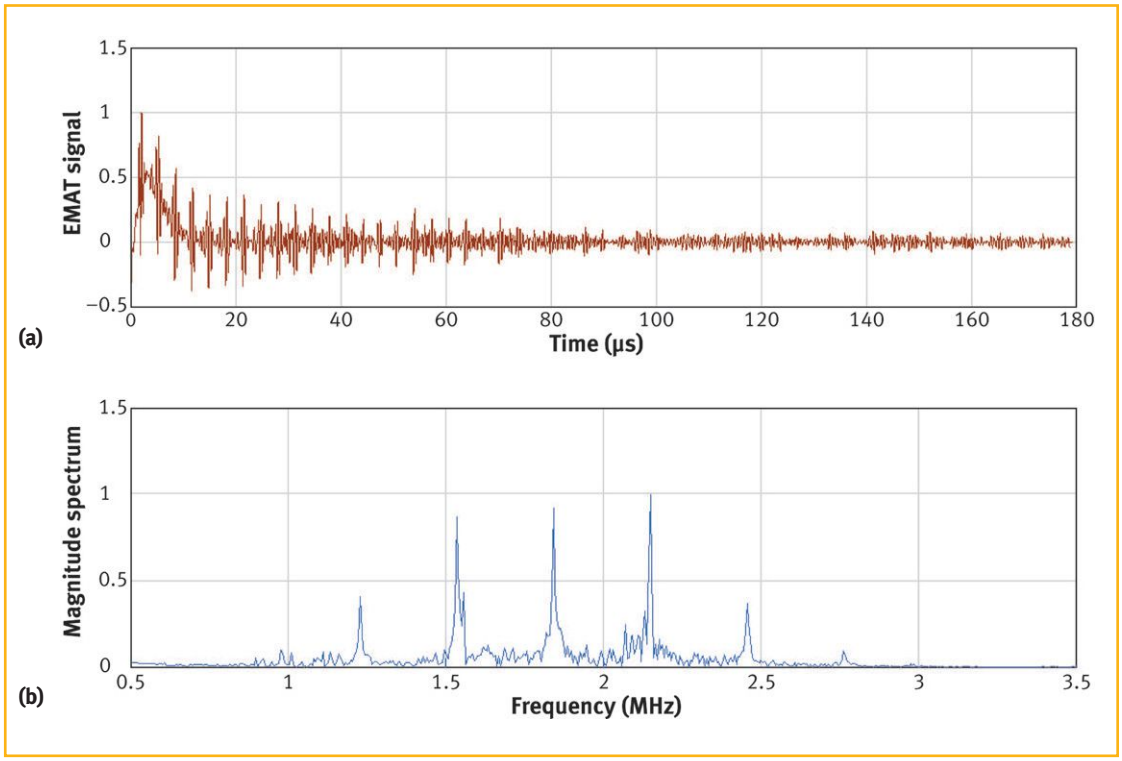

Figure 7. Normalized normal beam shear wave signal obtained on a 5.29 mm steel plate: (a) normal beam shear wave signal; and (b) fast fourier transform of normal beam shear wave signal.

known thickness. Sound velocity plays an essential role in thickness gauging. It is usually a required procedure to calibrate an ultrasonic thickness gauge to the sound speed in the material to be measured. The accuracy of the final measurement can be only as good as this calibration.

An 8-cycle tone burst with a center frequency of 1.85 MHz was used to excite the EMAT coil. The liftoff between the coil and the sample surface is about 1.0 mm. Figure 7 shows the received signal and its fast fourier transform (FFT). The FFT magnitude spectrum exhibits multiple sharp peaks, as predicted by Equation 3.

It is seen that the frequency interval, namely Δf, between the peaks is quite consistent from peak to peak. This will be the case as long as enough of the data points in the time domain are taken into account in the FFT process, ensuring an acceptable resolution in frequency. The measured plate thickness is calculated from Equation 4 to be 5.27 mm, using C_S = 3.240 mm/μs and the average frequency interval Δf = 0.3073 MHz from Table 1. The relative error in the measured thickness is about 0.4%. The same type of technique has been applied by other researchers to aluminum sheet thickness gauging, achieving a submicron accuracy with a relative error within 0.2% (Dixon et al. 2001).

Alternatively, if one uses the transit time technique as described in Equation 5, the transit time Δt can be extracted from the time trace of the EMAT signal to be 3.24 μs, giving a thickness of 5.25 mm. When measured directly from the raw data, the resolution of the transit time is limited by the sampling frequency of the digitizer, which is 50 MHz in this setup. As mentioned previously, the accuracy of thickness measurement can be improved by using a cross-correlation technique with curve fitting for finding the exact peak in the cross-correlation result.

TABLE 1
Peak frequencies f_{peak} from the FFT plot and calculated frequency interval Δf

	First peak	Second peak	Third peak	Fourth peak	Fifth peak
f_{peak} (MHz)	1.229	1.536	1.844	2.151	2.458
Δf (MHz)		0.307	0.308	0.307	0.307
n (calculated)	4	5	6	7	8

For optimal design and best use of EMAT thickness gauges, many practical factors need to be considered, such as acoustic properties of the test material (for example, scattering and attenuation), thickness range, surface curvature and roughness, temperature, accuracy requirements, and so on. Extensive discussion of how these factors affect the design and choice of EMAT thickness gauges is beyond the scope of this paper. It is worth mentioning that, in addition to bulk waves, guided waves (for example, lamb and shear horizontal guided waves) may also be used for thickness determination. However, the underlying physics is more complex.

Concluding Remarks

This paper summarized the basic operational principles of EMATs for generating normal beam bulk waves and illustrated their typical application using thickness gauging as an example. Although the approach adopted in explaining the principle is approximate in nature, it is still expected to provide the designers as well as users with essential elements for a good understanding of the NDE technique.

ACKNOWLEDGMENTS

The author would like to thank Bruce W. Maxfield for a number of helpful suggestions on this article.

REFERENCES

Krautkrämer, J., and H. Krautkrämer, 1983, *Ultrasonic Testing of Materials*, third edition, Springer-Verlag, Berlin.

Maxfield, B., and Z. Wang, 2018, "Electromagnetic Acoustic Transducers for Nondestructive Evaluation," in *ASM Handbook, Volume 17: Nondestructive Evaluation of Materials*, ed. A. Ahmad and L. J. Bond, ASM International, Materials Park, OH, pp. 214–237.

Thompson, R.B., 1990, "4 - Physical Principles of Measurements with EMAT Transducers," Ultrasonic Measurement Methods, Vol. 19, *Physical Acoustics*, ed. R.N. Thurston and A.D. Pierce, Academic Press, NY, pp. 157–200.

Dixon, S., C. Edwards, and S.B. Palmer, 2001, "High Accuracy Non-contact Ultrasonic Thickness Gauging of Aluminum Sheet using Electromagnetic Acoustic Transducers," *Ultrasonics*, Vol. 39, No. 6, pp. 445–453.